Journal of Power Sources 196 (2011) 313–324

Contents lists available at ScienceDirect

Journal of Power Sources

journal homepage: www.elsevier.com/locate/jpowsour

Energy management of fuel cell/solar cell/supercapacitor hybrid power source

Phatiphat Thounthong[a,*], Viboon Chunkag[b], Panarit Sethakul[a], Suwat Sikkabut[c], Serge Pierfederici[d], Bernard Davat[d]

[a] Department of Teacher Training in Electrical Engineering, King Mongkut's University of Technology North Bangkok, 1518, Piboolsongkram Road, Bangsue, Bangkok 10800, Thailand
[b] Department of Electrical Engineering, King Mongkut's University of Technology North Bangkok, 1518, Piboolsongkram Road, Bangsue, Bangkok 10800, Thailand
[c] Thai-French Innovation Institute, King Mongkut's University of Technology North Bangkok, 1518, Piboolsongkram Road, Bangsue, Bangkok 10800, Thailand
[d] Groupe de Recherche en Electrotechnique et Electronique de Nancy (GREEN: UMR 7037), Nancy Université, INPL-ENSEM, 2, Avenue de la Forêt de Haye, Vandœuvre-lés-Nancy, Lorraine 54516, France

ARTICLE INFO

Article history:
Received 19 October 2009
Received in revised form
14 December 2009
Accepted 18 January 2010
Available online 1 February 2010

Keywords:
Converter
Energy management
Fuel cell
Photovoltaic array
Supercapacitor
Voltage control

ABSTRACT

This study presents an original control algorithm for a hybrid energy system with a renewable energy source, namely, a polymer electrolyte membrane fuel cell (PEMFC) and a photovoltaic (PV) array. A single storage device, i.e., a supercapacitor (ultracapacitor) module, is in the proposed structure. The main weak point of fuel cells (FCs) is slow dynamics because the power slope is limited to prevent fuel starvation problems, improve performance and increase lifetime. The very fast power response and high specific power of a supercapacitor complements the slower power output of the main source to produce the compatibility and performance characteristics needed in a load. The energy in the system is balanced by d.c.-bus energy regulation (or indirect voltage regulation). A supercapacitor module functions by supplying energy to regulate the d.c.-bus energy. The fuel cell, as a slow dynamic source in this system, supplies energy to the supercapacitor module in order to keep it charged. The photovoltaic array assists the fuel cell during daytime. To verify the proposed principle, a hardware system is realized with analog circuits for the fuel cell, solar cell and supercapacitor current control loops, and with numerical calculation (dSPACE) for the energy control loops. Experimental results with small-scale devices, namely, a PEMFC (1200 W, 46 A) manufactured by the Ballard Power System Company, a photovoltaic array (800 W, 31 A) manufactured by the Ekarat Solar Company and a supercapacitor module (100 F, 32 V) manufactured by the Maxwell Technologies Company, illustrate the excellent energy-management scheme during load cycles.

1. Introduction

Currently, most of the energy demand in the world is met by fossil and nuclear power plants. A small part is drawn from renewable energy technologies such as wind, solar, fuel cell, biomass and geothermal energy [1,2]. Wind energy, solar energy and fuel cells have experienced a remarkably rapid growth in the past ten years [3–5] because they are pollution-free sources of power. Additionally, they generate power near the load centres, which eliminates the need to run high-voltage transmission lines through rural and urban landscapes.

The cost of solar photovoltaic and fuel cell electricity is still high [6–8]. Nevertheless, with ongoing research, development and utilization of these technologies around the world, the costs of solar cells and fuel cell energy are expected to fall in the next few years. As for solar cell and fuel cell electricity producers, they now sell power freely to end-users through truly open access to the transmission lines. For this reason, they are likely to benefit as much as other producers of electricity. Another benefit in their favour is that the cost of renewable energy falls as technology advances, whereas the cost of electricity from conventional power plants rises with inflation. The difference in their trends indicates that hydrogen and solar power will be more advantageous in future.

In the near future, the utility power system at a large scale will be supplied by renewable energy sources and storage device(s), i.e., *hybrid energy systems*, in order to increase their reliability and make them more effective. The specific properties of fuel cells and solar cells are as follows:

- The amount of power the fuel cell system delivers is controlled by the amount of current drawn from the system if the proper conditions for cell operation are maintained. When a large load is applied to the cells, the sudden increase in the current can cause the system to stall if the depleted oxygen or hydrogen cannot be replenished immediately and sufficiently. Cell starvation can lead to a system stall, permanent cell damage or

* Corresponding author. Tel.: +66 2 913 2500x3332; fax: +66 2 587 8255.
E-mail addresses: Phatiphat.Thounthong@ensem.inpl-nancy.fr, phtt@kmutnb.ac.th (P. Thounthong).

0378-7753/$ – see front matter © 2010 Elsevier B.V. All rights reserved.
doi:10.1016/j.jpowsour.2010.01.051

Nomenclature

a.c.	alternating current
d.c.	direct current
FC	fuel cell
PV	photovoltaic
SC	supercapacitor
C_{Bus}	total capacitance at d.c.-bus (F)
C_{SC}	total capacitance of supercapacitor module (F)
i_{Load}	d.c.-bus load current (A)
i_{FC}	fuel cell current (A)
i_{FCREF}	fuel cell current reference (set-point) (A)
i_{Sol}	solar cell (photovoltaic) current (A)
i_{SolREF}	solar cell current reference (set-point) (A)
i_{SC}	supercapacitor current (A)
i_{SCREF}	supercapacitor current reference (set-point) (A)
p_{Load}	load power (W)
p_{FC}	fuel cell power (W)
p_{FCa}	fuel cell output power to d.c.-bus (W)
p_{FCREF}	fuel cell power reference (set-point) (W)
p_{FCMax}	maximum fuel cell power (W)
p_{Sol}	solar cell (photovoltaic) power (W)
p_{Sola}	solar cell output power to d.c.-bus (W)
p_{SolREF}	solar cell power reference (set-point) (W)
p_{SolMax}	maximum solar cell power (W)
p_{SC}	supercapacitor power (W)
p_{SCa}	supercapacitor output power to d.c.-bus (W)
p_{SCREF}	supercapacitor power reference (set-point) (W)
p_{SCMax}	maximum supercapacitor power (W)
v_{Bus}	d.c.-bus voltage (V)
v_{FC}	fuel cell voltage (V)
v_{Sol}	solar cell (photovoltaic) voltage (V)
v_{SC}	supercapacitor voltage (V)
y_{Bus}	d.c.-bus energy (J)
y_{BusREF}	d.c.-bus energy reference (set-point) (J)
y_{SC}	supercapacitor energy (J)
y_{SCREF}	supercapacitor energy reference (set-point) (J)
y_T	total energy at d.c.-bus and supercapacitor (J)
r_{FC}	equivalent series resistance in fuel cell converter (Ω)
r_{Sol}	equivalent series resistance in solar cell converter (Ω)
r_{SC}	equivalent series resistance in supercapacitor converter (Ω)
$\boldsymbol{u}$	input variable vector
$\boldsymbol{x}$	state-variable vector
$\boldsymbol{y}$	output vector
$\varphi(\cdot)$, $\psi(\cdot)$, $\phi(\cdot)$	smooth mapping functions

reduced cell lifetime. To protect the fuel cells from overloading and starvation, especially during transient conditions, excessive oxygen and hydrogen can be supplied to the cells during the steady-state operation, which increases the reserve of available power in anticipation of a load increase. This strategy, however, is conservative and leads to increased parasitic losses, decreased air utilization and thereby compromised system performance. Therefore, the fuel cell power or current slope must be limited to prevent a fuel cell stack from experiencing the fuel starvation phenomenon and to optimize the system, for example, 4 A s^{-1} for a 0.5 kW, 12.5-V PEMFC [9], and 5, 10 and 50 A s^{-1} for a 20 kW, 48-V PEMFC [10].

- The output power of solar cells fluctuates considerably depending on solar radiation, weather conditions and temperature [11,12].

Therefore, in order to supply electric power to fluctuating loads with a hybrid system composed of the above-mentioned fuel cell and solar cell, an electric energy-storage system is needed to compensate for the gap between the output from the renewable energy sources and the load, in addition to the collaborative load sharing among those energies [13–15].

Moreover, hydrogen as an energy storage media has the potential to address both daily and seasonal buffering requirements. Systems that employ an electrolyzer to convert excess electricity to hydrogen coupled with hydrogen storage and regeneration using a fuel cell can, in principle, provide power with zero (or near zero) emissions. Hydrogen production by solar energy is a 'renewable–regenerative system' [4], and this process is known as the electrolysis process. The basic principle is the following: when the photovoltaic input power exceeds the load power demand, the system controller determines that the energy should be directed to hydrogen production. In this kind of operation, i.e., a solar-based renewable–regenerative system, almost half of the solar input energy is directed to hydrogen production and converted with 60% energy efficiency [4].

Based on present storage device technology, battery design has to supply the trade-off between specific energy, specific power and cycle life. The difficulty in obtaining high values of these three parameters has led to some suggestions that the energy-storage system of distributed generation systems should be a hybridization of an energy source and a power source [16,17]. The energy source, mainly fuel cells and solar cells in this study, has high specific energy, whereas the power source has high specific power. The power sources can be recharged from the main energy source(s) when there is less demand. The power source that has received wide attention is the supercapacitor (or 'ultracapacitor', or 'electrochemical double-layer capacitor') [18–20].

The enhancements in the performance of renewable energy source power systems that are gained by adding energy storage are all derived from the ability to shift the system output. Firming-up the renewable system is accomplished by ensuring that energy is available when there is a demand for it rather than being limited by the availability of the renewable resource. As a result, the system output may need to be shifted to periods when the hydrogen and/or the sun, for example, are not available [21]. Depending on the size and type of the energy-storage system and the load, it may be possible to provide all of the power needed to support the load. A much more common scenario is for the energy storage to simply provide enough power for applications, like peak shaving, without having full load support capability. The energy-storage system may also provide sufficient energy to ride out electric service interruptions that range from a few seconds to a few hours. This is especially important for service disruptions that occur when the renewable resource is not available.

In this study, a fuel cell/photovoltaic/supercapacitor hybrid power source is proposed. A power electronic converter structure, energy management and innovative energy control law are presented. To authenticate the proposed principle, the hardware system is realized by analog circuits and digital estimation with a dSPACE controller. Experimental results obtained with small-scale devices illustrate the system performance.

2. Renewable energy hybrid system

2.1. System configuration

The power converter structure of the system is shown in Fig. 1. Fuel cell and solar cell power-generating systems may provide direct or alternating current (d.c. or a.c.) to satisfy application-specific power needs (Fig. 1). The current, voltage and power quality

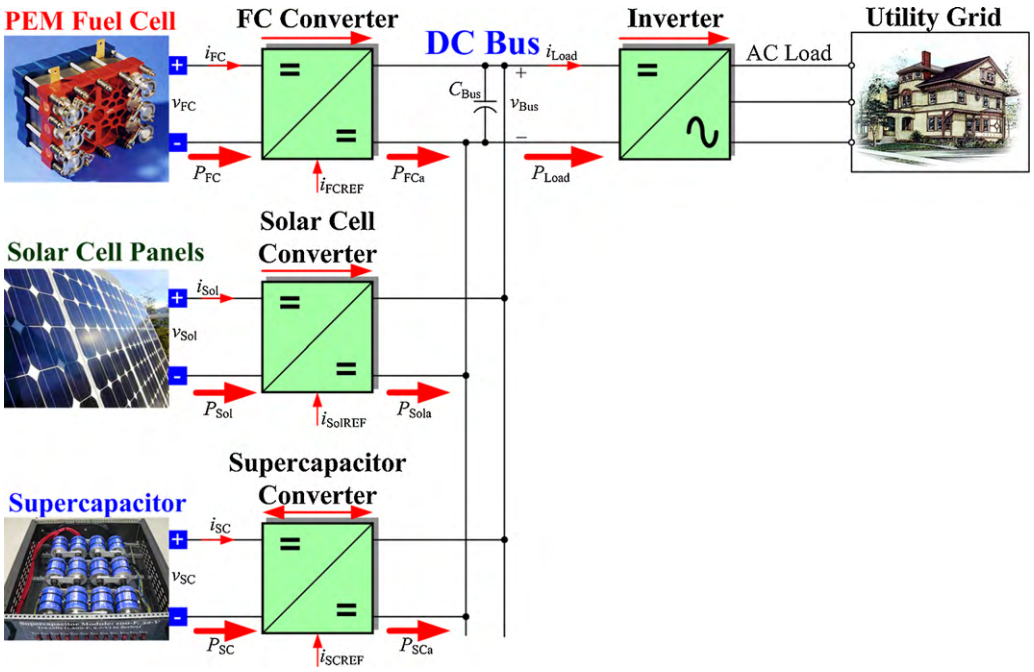

Fig. 1. Proposed hybrid energy system supplied by fuel cell, solar cell and supercapacitor, where p_{Load} ($= v_{Bus} \times i_{Load}$), v_{Bus} and i_{Load} are load power, d.c.-bus voltage and d.c.-bus load current, respectively. p_{FC} ($= v_{FC} \times i_{FC}$), v_{FC} and i_{FC} are fuel cell power, voltage and current, respectively. p_{Sol} ($= v_{Sol} \times i_{Sol}$), v_{Sol} and i_{Sol} are solar cell power, voltage and current, respectively. p_{SC} ($= v_{SC} \times i_{SC}$), v_{SC} and i_{SC} are supercapacitor power, voltage, and current, respectively. p_{FCa}, p_{Sola} and p_{SCa} are the output powers to d.c. link from converters of fuel cell, solar cell and supercapacitor, respectively. i_{FCREF}, i_{SolREF}, i_{SCREF} are the current references of the fuel cell, solar cell and supercapacitor converters, respectively.

are controlled by electronic power-conditioning systems. Generally, voltage regulators and d.c.–d.c. converters (chopper circuits) are used to control and adjust the fuel cell and photovoltaic d.c. output voltages to useful values [22,23].

The voltages of the fuel cell and solar cell vary with the current drawn by the load and decrease significantly at high load currents [24]. Therefore, a power-electronics system is needed to process the raw output power from the stack or panel and provide power to the load at a constant d.c. or a.c. voltage. Typically, the power-electronics systems include multiple interconnected power converters: for example, a d.c.–d.c. converter is often followed by a d.c.–a.c. converter for stationary applications [25]. The switching scheme in such power converters can be based on pulse-width modulation (PWM), resonant, quasi-resonant, soft-switched, or line-commutated switching [26–28]. Furthermore, the topological structures of these converters can vary dramatically [29].

The supercapacitor bank is always connected to the d.c.-bus by means of a two-quadrant d.c.–d.c. converter (bidirectional converter), a 'supercapacitor converter'. The supercapacitor power can be positive or negative, which allows energy to be transferred in both directions [30].

An inverter is used to convert the d.c. voltage to a useful a.c. voltage. It may operate as grid-independent or with grid-synchronization. Then, the solar cell supplies all its output power to the d.c.-bus, and the fuel cell supplies a slowly fluctuating power difference between the load power p_{Load} demand and the solar cell output power. A supercapacitor storage device can compensate for both a sudden change in the load demand and rapidly fluctuating solar cell output power caused by solar radiation; therefore, the load is supplied with stable power.

As depicted in Fig. 1, the proposed system has a multi-source structure (or cascade scheme). The cascaded structure can lead to interactions between converters that cause the system to be unstable, if they are designed separately. This problem has been studied during the past decade. In this case, to study interactions between the converters, impedance criteria are often used to determine the stability of the cascaded system. Nonetheless, the technique only proves the asymptotic stability around a given operating point. The large signal stability properties or the behaviour of the system in the case of outsized disturbances are not considered in this model. In this paper, a non-linear control algorithm based on the differential flatness principle of the renewable power plant is proposed. Design controller parameters are independent of the operating point. Interactions between the converters are taken into account by the controllers, and high dynamics in perturbation rejection are accomplished.

2.2. Energy management

For reasons of safety and dynamics, the fuel cell, solar cell and supercapacitor converters are usually controlled primarily by inner current-regulation loops [17]. The dynamics of current-regulation loops are much faster than those of outer control loops, which are described later. Therefore, the fuel cell current i_{FC}, the solar cell current i_{Sol} and the supercapacitor current i_{SC} are considered to follow their references i_{FCREF}, i_{SolREF} and i_{SCREF} perfectly.

Energy management of multi-power sources has already been studied recently, for example, Feroldi et al. [31] studied control (based on efficiency map) of a fuel cell/supercapacitor hybrid power source for vehicle applications, Payman et al. [32] studied control of a regulated d.c. voltage supplied by a fuel cell and supercapacitor storage device based on a differential flatness system, and Thounthong et al. addressed a regulated d.c.-bus voltage fuel cell/supercapacitor hybrid source [33], a regulated d.c.-bus voltage fuel cell/battery/supercapacitor hybrid source [34] and an unregulated d.c.-bus voltage fuel cell/battery hybrid source [14].

Thus, in the proposed system depicted in Fig. 1, there are two-voltage variables, or two-energy variables, to be regulated. The d.c.-bus energy y_{Bus} is the most important variable, and the supercapacitor storage energy y_{SC} is the next most important. Therefore, based on the previous work described above, it is proposed to utilize supercapacitors, which are the fastest energy source in the pro-

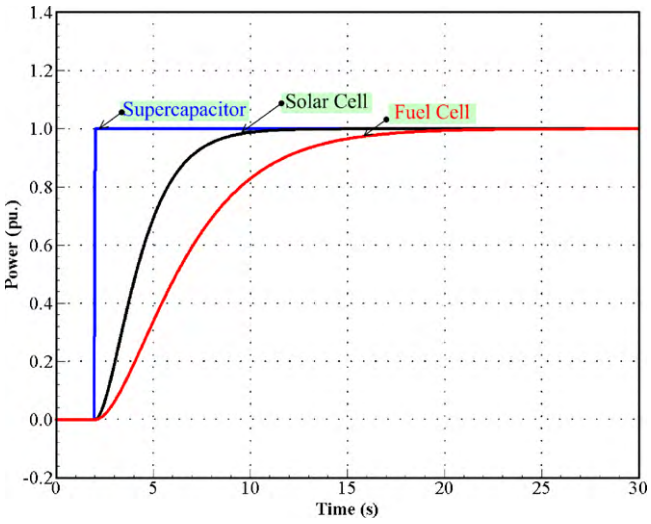

Fig. 2. Dynamic classification for proposed hybrid power source.

posed system, to supply the energy for the d.c.-bus [33,34]. Thus, the fuel cell (as the slowest dynamic device) and solar cell supply energy for both the d.c.-bus capacitor C_{Bus} and the supercapacitors C_{SC} to keep them charged.

At the d.c. link, there are three sources that supply energy at the same time. Therefore, the dynamics of the three sources must be classified in order to guarantee system stability [34], as illustrated in Fig. 2. Note that the power unit in Fig. 2 is the normalized unit (or per-unit [pu]). Thus, the defined dynamic classification depicted in Fig. 2 is obtained from the simulation result using Matlab–Simulink, and the experimental results of the power source dynamics are presented after the performance validation section. The supercapacitor is operated as the highest dynamic power source to provide the micro-cycles and the fast dynamic power supply. It can withstand a very large number of charge–discharge cycles without degradation (or virtually infinite cycles) [33,35]. The fuel cell generator is operated as the lowest dynamic power source. The fuel cell current or power slope must be limited to avoid the fuel starvation phenomenon. The fuel cell limited current or power slope has been experimentally determined to be the highest slope of an operating fuel cell system, where no fuel starvation occurs in order to improve its lifetime [33,34]. The photovoltaic generator is between the fuel cell and supercapacitor in the dynamic classification.

2.2.1. Principle of differential flatness theory

A non-linear control algorithm based on the flatness properties [36–38] of the system is proposed. According to the flatness-control law, the tuning controller parameters are independent of the operating point [32]. According to Fliess et al. [39,40], an independent dynamic system is considered to be differentially flat if an output $\boldsymbol{y}$ is given by:

$$\boldsymbol{y} = \phi(\boldsymbol{x}, \boldsymbol{u}, \dot{u}, \ldots, u^{(\alpha)}), \quad \boldsymbol{y} \in \Re^{m} \tag{1}$$

such that the state $\boldsymbol{x}$ and controls $\boldsymbol{u}$ (or inputs) can be written as:

$$\boldsymbol{x} = \varphi(\boldsymbol{y}, \dot{y}, \ldots, y^{(\beta)}), \quad \boldsymbol{x} \in \Re^{n} \tag{2}$$

$$\boldsymbol{u} = \psi(\boldsymbol{y}, \dot{y}, \ldots, y^{(\beta+1)}), \quad \boldsymbol{u} \in \Re^{m} \tag{3}$$

where $\varphi(\cdot), \psi(\cdot), \phi(\cdot)$ are the smooth mapping functions, α and β are a finite number of their time derivatives, and $(n, m) \in \mathbb{N}$. Moreover, it is assumed that $m \leq n$.

The output $\boldsymbol{y}$ is called a *flat output*. Thus, a dynamic system is, in nature, differentially flat if it is equivalent to a system without dynamics, i.e., a static system. In other words, there are no differential constraints in output space. The apparent advantage of a differentially flat system is that every trajectory in the output space is feasible; therefore, trajectory generation is theoretically simpler in terms of the flat outputs. For this reason, by using the flatness estimation in power electronic applications, interactions between the converters are taken into account by the flatness-control law and high dynamics in perturbation elimination are achieved.

2.2.2. d.c.-Bus energy control

Based on the flatness-control, the electrostatic energy y_{Bus} stored in the total d.c.-bus capacitor C_{Bus} is considered as the flat output variable (Eq. (1)), i.e.:

$$y_{Bus} = \frac{1}{2} C_{Bus} v_{Bus}^2 \tag{4}$$

It is assumed that the supercapacitor current follows its reference value perfectly. Thus:

$$i_{SC} = i_{SCREF} = \frac{p_{SC}}{v_{SC}} = \frac{p_{SCREF}}{v_{SC}} \tag{5}$$

where p_{SCREF} is the control variable of the reduced system described in Eq. (3).

Therefore, the state variable v_{Bus} may be put into a form similar to that in Eq. (2):

$$v_{Bus} = \sqrt{\frac{2y_{Bus}}{C_{Bus}}} = \varphi_1(y) \tag{6}$$

To obtain a relationship between the control variable p_{SC} and the flat output variable y_{Bus}, the differential equation verified by the reduced model from Fig. 1 is written as:

$$\dot{y}_{Bus} = p_{FCa} + p_{Sola} + p_{SCa} - p_{Load} \tag{7}$$

where

$$p_{FCa} = p_{FC} - r_{FC}\left(\frac{p_{FC}}{v_{FC}}\right)^2 \tag{8}$$

$$p_{Sola} = p_{Sol} - r_{Sol}\left(\frac{p_{Sol}}{v_{Sol}}\right)^2 \tag{9}$$

$$p_{SCa} = p_{SC} - r_{SC}\left(\frac{p_{SC}}{v_{SC}}\right)^2 \tag{10}$$

r_{FC} is the total equivalent series resistance in the fuel cell converter. Here, only static resistance loss is considered [32]. r_{Sol} is the total equivalent series resistance in the solar cell converter. r_{SC} is the total equivalent series resistance in the supercapacitor converter.

It follows that:

$$p_{SCREF} = 2p_{SCMax}\left[1 - \sqrt{1 - \left(\frac{\dot{y}_{Bus} + p_{Load} - p_{FCa} - p_{Sola}}{p_{SCMax}}\right)}\right] = \psi_1(y, \dot{y}) \tag{11}$$

where

$$p_{SCMax} = \frac{v_{SC}^2}{4r_{SC}} \tag{12}$$

$$p_{Load} = v_{Bus} i_{Load} = \sqrt{\frac{2y_{Bus}}{C_{Bus}}}\, i_{Load} \tag{13}$$

p_{SCMax} is the limited maximum power from the supercapacitor module.

Thus, it is apparent that $p_{SC} = \psi_1(y, \dot{y})$, which corresponds with Eq. (3), and the proposed reduced system with the control variable p_{SC} can be considered to be a flat system associated with y_{Bus} as the flat output variable.

To ensure the control of the flat output variable y_{Bus} to its reference trajectory y_{BusREF}, the following control law is based on the

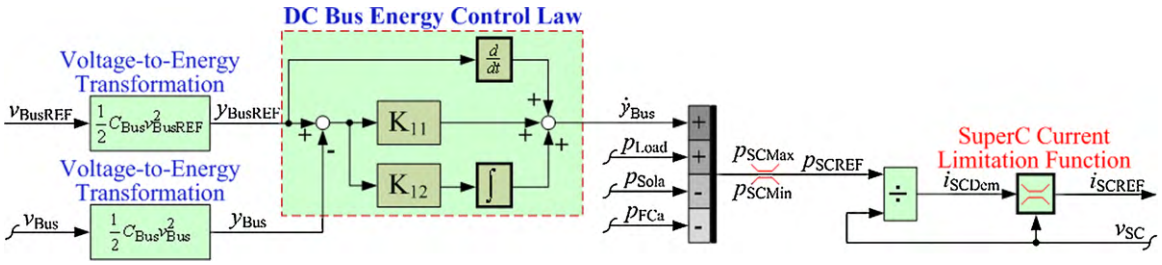

Fig. 3. Proposed d.c.-bus energy control loop for fuel cell/solar cell/supercapacitor hybrid source.

well-known second-order control law:

$$(\dot{y}_{Bus} - \dot{y}_{BusREF}) + K_{11}(y_{Bus} - y_{BusREF}) + K_{12}\int_0^t (y_{Bus} - y_{BusREF})\,d\tau = 0 \quad (14)$$

where K_{11}, and K_{12} are the controller parameters. Defining $e_{yBus} = y_{Bus} - y_{BusREF}$, $K_{11} = 2\zeta\omega_n$, and $K_{12} = \omega_n^2$ gives:

$$\ddot{e}_{yBus} + 2\zeta\omega_n\dot{e}_{yBus} + \omega_n^2 e_{yBus} = 0 \quad (15)$$

It is obvious that the control system is stable for K_{11}, $K_{12} > 0$. Based on the power electronic constant switching frequency f_S and a cascade control structure, the outer control loop (here the d.c.-bus energy control) must operate at a cut-off frequency $f_e \ll f_C$ (a cut-off frequency of the supercapacitor current loop or power loop) $\ll f_S$ [41]. The d.c.-bus energy control loop detailed above is portrayed in Fig. 3.

The d.c.-bus energy control law generates a supercapacitor power reference p_{SCREF}. This signal is then divided by the measured supercapacitor voltage v_{SC} and limited to maintain the supercapacitor voltage within an interval $[V_{SCMin}, V_{SCMax}]$ by limiting the supercapacitor charging current or discharging current, as presented in the block "SuperC Current Limitation Function" [33]. The higher voltage value V_{SCMax} of this interval corresponds to the maximum voltage of the storage device. Generally, the lower voltage value V_{SCMin} is chosen as $V_{SCMax}/2$, which causes only 25% of the energy in the supercapacitor bank to remain [33]; as a result, the supercapacitor discharge becomes ineffective. This results in the supercapacitor current reference i_{SCREF}.

2.2.3. Supercapacitor energy control

The classical electrostatic energy storage y_{SC} in the supercapacitor is expressed by:

$$y_{SC} = \frac{1}{2}C_{SC}v_{SC}^2 \quad (16)$$

where C_{SC} is the supercapacitor capacitance (refer to Fig. 1), and v_{SC} is the supercapacitor voltage.

Again, based on the flatness-control, the total electrostatic energy y_T stored in the total d.c.-bus capacitor C_{Bus} and the supercapacitor C_{SC} is taken as the flat output variable (Eq. (1)), i.e.:

$$y_T = y_{Bus} + y_{SC} = \frac{1}{2}C_{Bus}v_{Bus}^2 + \frac{1}{2}C_{SC}v_{SC}^2 \quad (17)$$

It is again assumed that the fuel cell and photovoltaic currents follow their reference values perfectly. Thus:

$$i_{FC} = i_{FCREF} = \frac{p_{FC}}{v_{FC}} = \frac{p_{FCREF}}{v_{FC}} \quad (18)$$

$$i_{Sol} = i_{SolREF} = \frac{p_{Sol}}{v_{Sol}} = \frac{p_{SolREF}}{v_{Sol}} \quad (19)$$

where p_{FCREF} and p_{SolREF} are the control variables of the reduced system (Eq. (3)).

Thus, the state variable v_{SC} may be put into a form similar to that of Eq. (2):

$$v_{SC} = \sqrt{\frac{2(y_T - y_{Bus})}{C_{SC}}} = \varphi_2(y) \quad (20)$$

The differential equation verified by the reduced model from Fig. 1 is:

$$\dot{y}_T = p_{Ta} - p_{Load} \quad (21)$$

where

$$p_{Ta} = p_{FCa} + p_{Sola} = p_T - r_T\left(\frac{p_T}{v_T}\right)^2 \quad (22)$$

For a fuel cell and a solar cell that are combined as an energy source to supply energy to a d.c.-bus and supercapacitor, v_T is defined as presented in Eq. (22) and r_T represents the total losses in the fuel cell and photovoltaic converters.

Therefore:

$$p_{TREF} = 2p_{TMax}\left[1 - \sqrt{1 - \left(\frac{\dot{y}_T + p_{Load}}{p_{TMax}}\right)}\right] = \psi_2(y, \dot{y}) \quad (23)$$

where

$$p_{TMax} = \frac{v_T^2}{4r_T} \quad (24)$$

In fact:

$$p_{TMax} = p_{FCMax} + p_{FCMax} \quad (25)$$

p_{FCMax} is the maximum fuel cell power. p_{SolMax} is the maximum photovoltaic power.

Photovoltaic power systems require some specific estimation algorithms to deliver the maximum power point (MPP) because the output features of a solar cell vary with environmental changes in irradiance and temperature. Many previous investigations have presented different techniques for maximum power point tracking (MPPT) of photovoltaic arrays [42–44]. It is beyond the scope of this study to present the MPPT algorithm here, though it is similar to Eq. (14). Because the supercapacitor energy storage has a large capacity and the supercapacitor energy is defined as a slower dynamic variable than the d.c.-bus energy variable, the total (supercapacitor) energy control law is defined as:

$$(\dot{y}_T - \dot{y}_{TREF}) + K_{21}(y_T - y_{TREF}) = 0 \quad (26)$$

The supercapacitor energy control loop is shown in Fig. 4. The total energy control law generates a total power reference p_{TREF}. First, p_{TREF} is considered to be the photovoltaic power reference $p_{SolarREF}$. It must be limited in level, within an interval maximum $p_{SolarMax}$ (MPP) and minimum $p_{SolarMin}$ (set to 0 W), and have limited dynamics to respect constraints in the dynamic classification (Fig. 2). Here, the second-order delay [34] is selected as a photovoltaic power dynamic limitation, as illustrated in Fig. 4. Second, the difference between the total power reference p_{TREF} and the

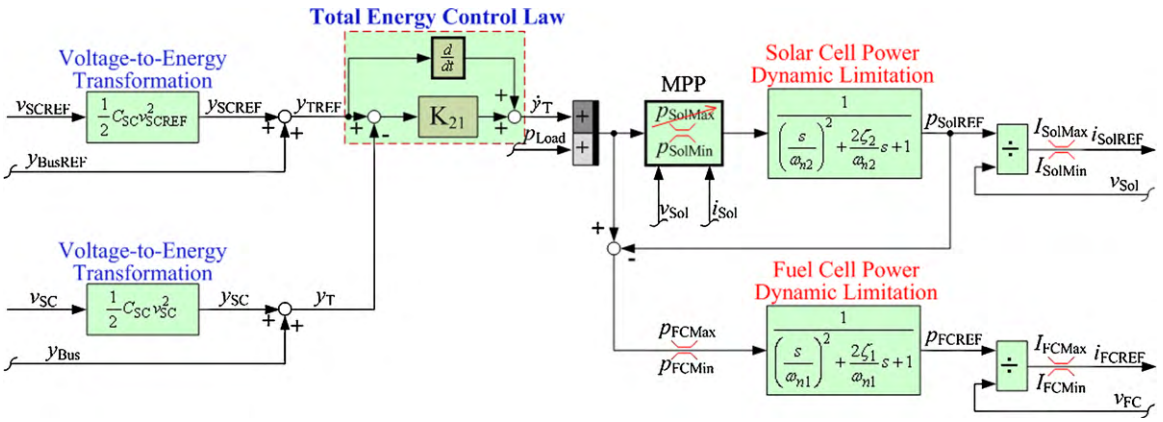

Fig. 4. Proposed supercapacitor energy control loop for fuel cell/solar cell/supercapacitor hybrid source.

photovoltaic power reference $p_{SolarREF}$ is the fuel cell power reference p_{FCREF}. It must be limited in level, within an interval maximum p_{FCMax} and minimum p_{FCMin} (set to 0 W), and be limited in dynamics to respect the dynamic classification constraints in Fig. 2. Again, second-order delay is selected as a fuel cell power dynamic limitation.

3. Performance validation

3.1. Test bench description

In order to authenticate the proposed original hybrid energy management, a small-scale test bench has been implemented, as presented in Fig. 5. The fuel cell system used in this effort is a Ballard Nexa fuel cell system (1.2 kW, 46 A). It is supplied using pure hydrogen with a regulated pressure of 10 bar from bottles under a pressure of 150 bar and with clean dry air from a compressor. The photovoltaic array (800 W, 31 A) was obtained by connecting four panels (200 W, 7.78 A) in series. The solar cell panels were developed and manufactured by the Ekarat Solar Company. They were installed on the roof of the laboratory building, as illustrated in Fig. 5. The supercapacitor module (100 F, 32 V, based on Maxwell Technologies Company) was obtained by connecting 12 cells BCAP1200 (capacitance: 1200 F; maximum voltage: 2.7 V) in series, as shown in Fig. 5.

The fuel cell converter (1200 W) is composed of four-phase boost converters connected in parallel using the interleaving technique [45] and is selected to adapt the low d.c. voltage delivered by the fuel cell, which is approximately 26 V at rated power, to the 60 V d.c.-bus. Thus, each boost converter is composed of a high-frequency input inductor (420 μH), four output filtering capacitors connected in parallel (each capacitor is an aluminum electrolytic capacitor (470 μF), thus the total capacitance is 1880 μF), a diode (Schottky diode RURG3020: 200 V, 30 A), and a main power switch (power metal–oxide–semiconductor field-effect transistor IRFP264N MOSFET: 250 V, 38 A). The frequency of the pulse-width modulation (PWM) that drives each boost converter is 25 kHz.

The solar cell converter (800 W) is composed of two-phase boost converters connected in parallel by the interleaving technique and is selected to adapt the low d.c. voltage delivered by the solar panels, which is approximately 25 V at rated power, to the 60 V d.c.-bus. Thus, each boost converter is composed of a high-frequency input inductor (140 μH), four output filtering capacitors connected in parallel (total capacitance: 4400 μF), a diode (Schottky diode RURG3020: 200 V, 30 A), and a main power switch (power metal–oxide–semiconductor field-effect transistor IRFP264N MOSFET: 250 V, 38 A). The frequency of the PWM that drives each boost converter is 25 kHz.

The supercapacitor converter is composed of four-phase bidirectional converters connected in parallel by the interleaving technique. Thus, each two-quadrant converter is composed of a high-frequency input inductor (290 μH), an output filtering capacitor (aluminum electrolytic capacitors: 680 μF), two power switches (power metal–oxide–semiconductor field-effect transistor IRFP264N MOSFET: 250 V, 38 A), and two diodes (Schottky diode RURG3020: 200 V, 30 A). The frequency of the PWM that drives

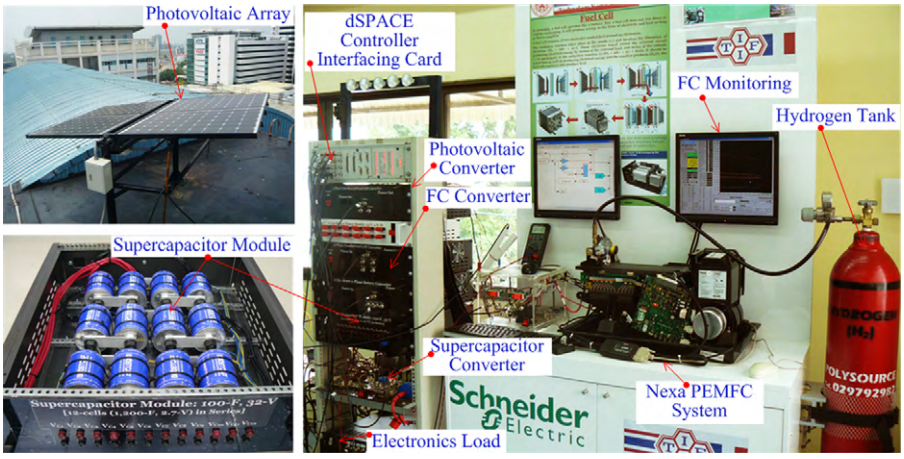

Fig. 5. Hybrid power source test bench.

Table 1
d.c.-bus energy control loop parameters.

Parameter	Value	
v_{BusREF}	60	V
C_{Bus}	12,200	μF
K_{11}	450	rad s^{-1}
K_{12}	22,500	rad s^{-2}
r_{FC}	0.14	Ω
r_{Sol}	0.12	Ω
r_{SC}	0.10	Ω
V_{SCMax}	32	V
V_{SCMin}	15	V
$I_{SCRated}$	150	A

Table 2
Supercapacitor energy control loop parameters.

Parameter	Value	
v_{SCREF}	25	V
C_{SC}	100	F
K_{21}	0.1	W J^{-1}
p_{SolMax} (rated)	800	W
p_{SolMin}	0	W
I_{SolMax} (rated)	28	A
I_{SolMin}	0	A
ζ_2	1	
ω_{n2}	0.8	rad s^{-1}
p_{FCMax}	500	W
p_{FCMin}	0	W
I_{FCMax} (rated)	46	A
I_{FCMin}	0	A
ζ_1	1	
ω_{n1}	0.4	rad s^{-1}

each bidirectional converter is 25 kHz. The supercapacitor current, which flows across the storage device, can either be positive or negative, which allows energy to be transferred in both directions.

3.2. Control description

Measurements of the fuel cell current i_{FC}, the solar cell current i_{Sol}, the supercapacitor current i_{SC}, the load current i_{Load}, the d.c. link voltage v_{Bus}, the fuel cell voltage v_{FC}, the solar cell voltage v_{Sol}, and the supercapacitor voltage v_{SC} are collected with zero-flux Hall effect sensors.

The fuel cell, the solar cell and the supercapacitor current-regulation loops were realized by analog circuits to function at a high bandwidth. Parameters associated with the d.c.-bus energy regulation loop and the supercapacitor energy regulation loop can be seen in Tables 1 and 2, respectively. The fuel cell power dynamic delay is shown in Table 2; this value was experimentally determined as the highest power slope of the FC system, where no fuel starvation occurs. It must be noted here that, for the small-test bench, the fuel cell maximum power p_{FCMax} is set at 500 W; but, the rated fuel cell power considered here is 1200 W. Further, these two energy control loops, which generate current references i_{FCREF}, i_{SolREF} and i_{SCREF} are implemented on the real time card dSPACE DS1104 through the mathematical environment of Matlab–Simulink with a sampling frequency of 25 kHz.

3.3. Experimental results

The studied d.c.-bus of 60 V is only connected to an electronic load. To validate the dynamics of the power (current) regulation loops for each power source, Figs. 6–8 present waveforms that are obtained during the stepped power demand. Fig. 6 illustrates the fuel cell power demand, power response, voltage and current. Fig. 7 contains the photovoltaic power demand, power response,

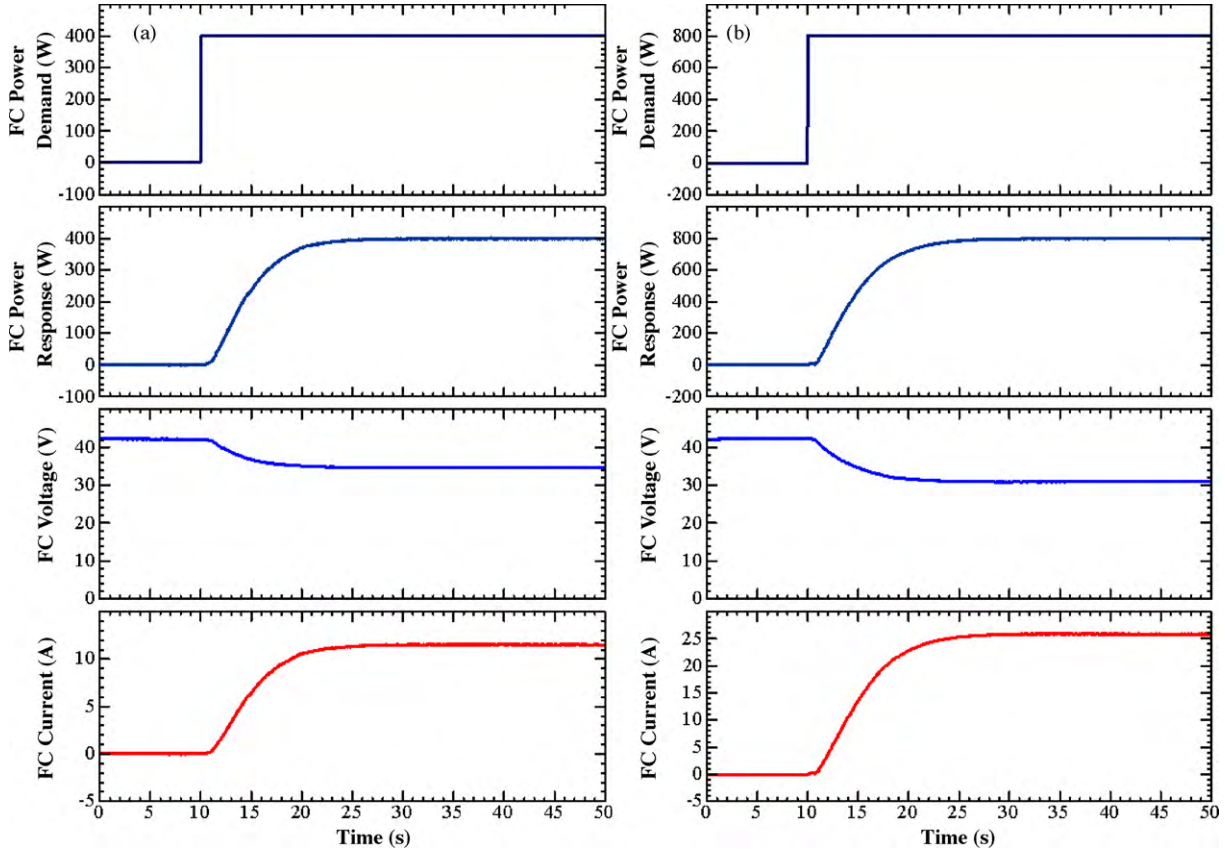

Fig. 6. Dynamic identification of fuel cell power control loop.

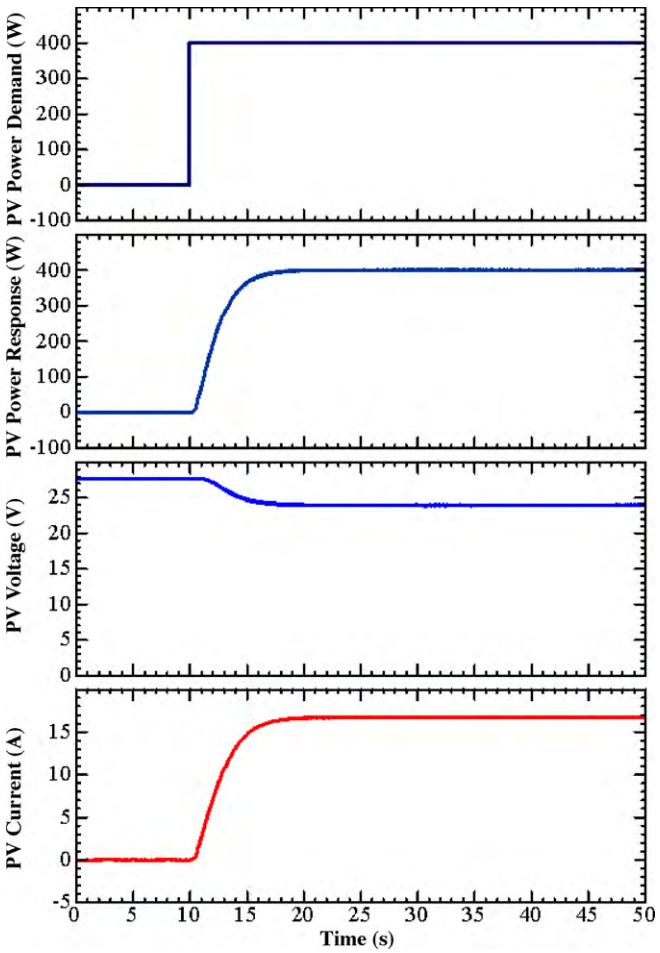

Fig. 7. Dynamic identification of photovoltaic power control loop.

voltage and current. Finally, Fig. 8 illustrates the supercapacitor power demand, power response, voltage and current. Because the fuel cell and photovoltaic powers are intentionally limited by the control algorithm (refer to Fig. 4: 'solar cell dynamic power limitation' and 'fuel cell power dynamic limitation'), a smooth transition of the power responses of the fuel cell and photovoltaic sources is observed, while the supercapacitor power dynamics are very fast. The supercapacitor can supply power from 0 to 400 W in 50 ms. It is clear that the fast response of the supercapacitor storage device can be operated with the fuel cell and solar cell main generators in order to improve system performance. The data in Fig. 6 also confirm that the fuel cell is controlled to avoid the fuel starvation phenomenon.

Because flatness-based control is model-based, it may have some sensitivity to errors in the model parameters. To authenticate its robustness, the flatness-based control was tested with the exact model parameters ($r_{FC} = 0.14\,\Omega, r_{Sol} = 0.12\,\Omega, r_{SC} = 0.10\,\Omega$) and in the lossless parameters case ($r_{FC} = 0\,\Omega, r_{Sol} = 0\,\Omega, r_{SC} = 0\,\Omega$). In the case of no losses, this leads to a drastically less complex estimation of the control law (Eqs. (8)–(11)). Comparisons (robustness) between the accurate parameters and the error parameters are given in Fig. 9. They generate waveforms that are obtained during the large load step from 0 to 500 W and show the d.c.-bus voltage, the load power (disturbance), the supercapacitor power, and the supercapacitor voltage (storage *SOC*). Because the power of the fuel cell and the solar cells are intentionally limited, the supercapacitor supplies the transient load power demand. Similar waveforms are seen in Fig. 9(a) and (b). The d.c.-bus voltage (d.c. link stabilization) is minimally influenced by the large step in load power. Clearly the performance of the control system is hardly affected by the considered error in model parameters. Experimental testing demonstrates that errors in these parameters have relatively little effect on regulation performance. It is therefore conclude that the non-linear differential flatness-based approach provides an absolutely robust controller in this application.

Waveforms obtained during the large load cycle are presented in Fig. 10. The data show the d.c.-bus voltage, the fuel cell voltage, the photovoltaic voltage, the load power, the supercapacitor power, the fuel cell power, the photovoltaic power, the supercapacitor current, the fuel cell current, the photovoltaic current, and the supercapacitor voltage (or the supercapacitor *SOC*). In the initial state, the small load power is equal to 100 W, and the storage device is fully charge, i.e., $v_{SC} = 25$ V; as a result, both the fuel cell and supercapacitor powers are zero, and the photovoltaic source supplies power for the load of 100 W. At $t = 40$ s, the load power steps to the final constant power of around 900 W (positive load power transition). The following observations are made:

- The supercapacitor supplies most of the 900 W power that is required during the transient step load.
- Simultaneously, the photovoltaic power increases with limited dynamics to a maximum power point (MPP) of around 300 W, which is limited by the maximum power point tracker (MPPT).
- Concurrently, the fuel cell power increases with limited dynamics to a maximum power of 500 W.
- The input from the supercapacitor, which supplies most of the transient power that is required during the stepped load, slowly decreases and the unit remains in a discharge state after the load step because the steady-state load power (approximately 900 W) is greater than the total power supplied by the fuel cell and photovoltaic array.

At $t = 100$ s, the supercapacitor voltage is equal to 19 V. As a result, the supercapacitor supplies its stored energy y_{SC} to the d.c.-bus. This energy y_{SC_Supply} is estimated to be:

$$y_{SC\_Supply} = \frac{1}{2}C_{SC}v_{SC}^2(t = 40\,\text{s}) - \frac{1}{2}C_{SC}v_{SC}^2(t = 100\,\text{s}) = 13.20\,\text{kJ} \quad (27)$$

The load power is reduced from the high constant power of 900 W to the low constant power of 100 W (negative load power transition). As a result, the supercapacitor changes from discharging to charging and demonstrates the following four phases:

- First, the fuel cell and photovoltaic array still supply their constant maximum powers to drive the load and to charge the supercapacitor.
- Second, at $t = 110$ s, the supercapacitor is approaching full charge, i.e., $v_{SC} = 23$ V. Consequently, the fuel cell power is reduced with limited power dynamics.
- Third, at $t = 120$ s, the supercapacitor is nearly fully charged, i.e., $v_{SC} = 24$ V. As a result, the photovoltaic power is reduced with limited power dynamics.
- Fourth, at $t = 160$ s, the supercapacitor is fully charged, i.e., $v_{SC} = v_{SCREF} = 25$ V. After slowly decreasing, the photovoltaic power remains at a constant power of 100 W for the load power demanded. Furthermore, the fuel cell and supercapacitor powers are zero.

It is evident that the d.c.-bus voltage waveform is stable during the large load cycle, which is critically important when employing supercapacitors to improve the dynamic performance of the whole system using the proposed control law.

Finally, Fig. 11 presents waveforms that are obtained during the long load cycles measured on 5 December, 2009. The waveforms are

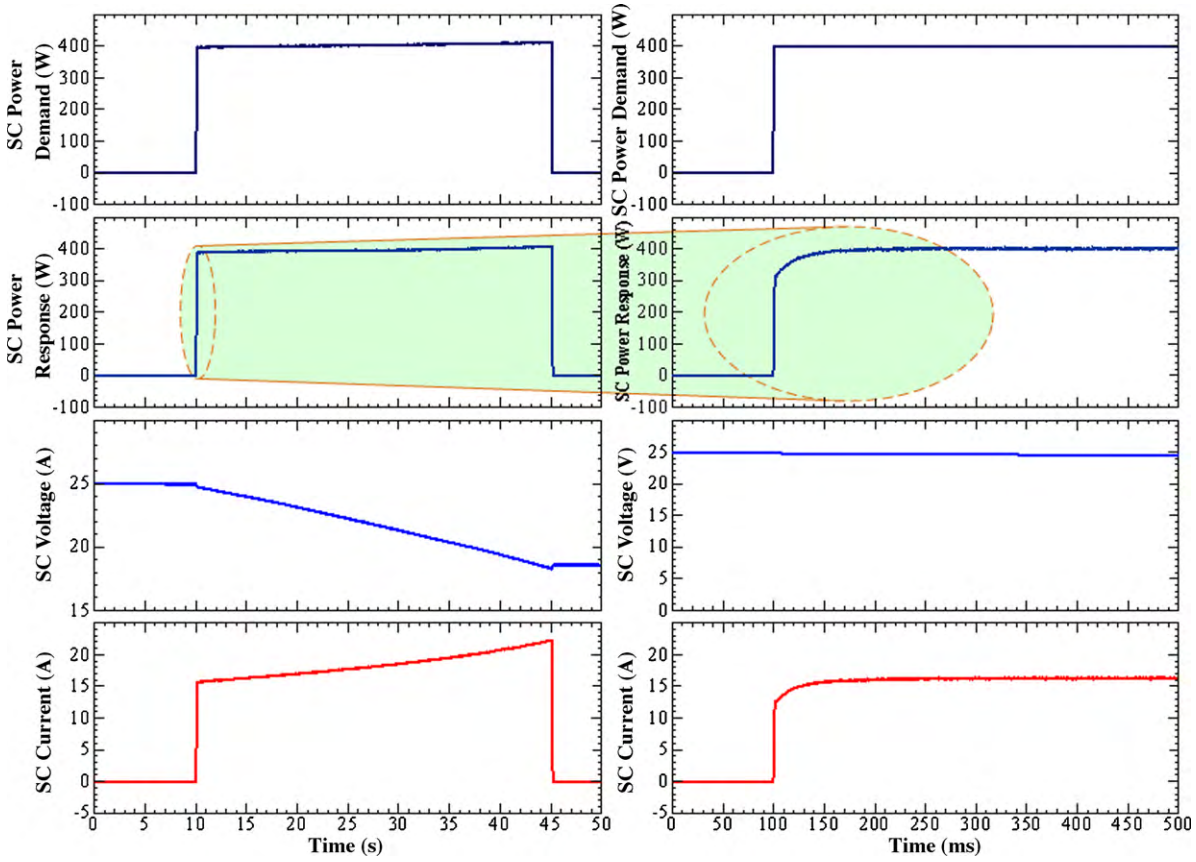

Fig. 8. Dynamic identification of supercapacitor power control loop.

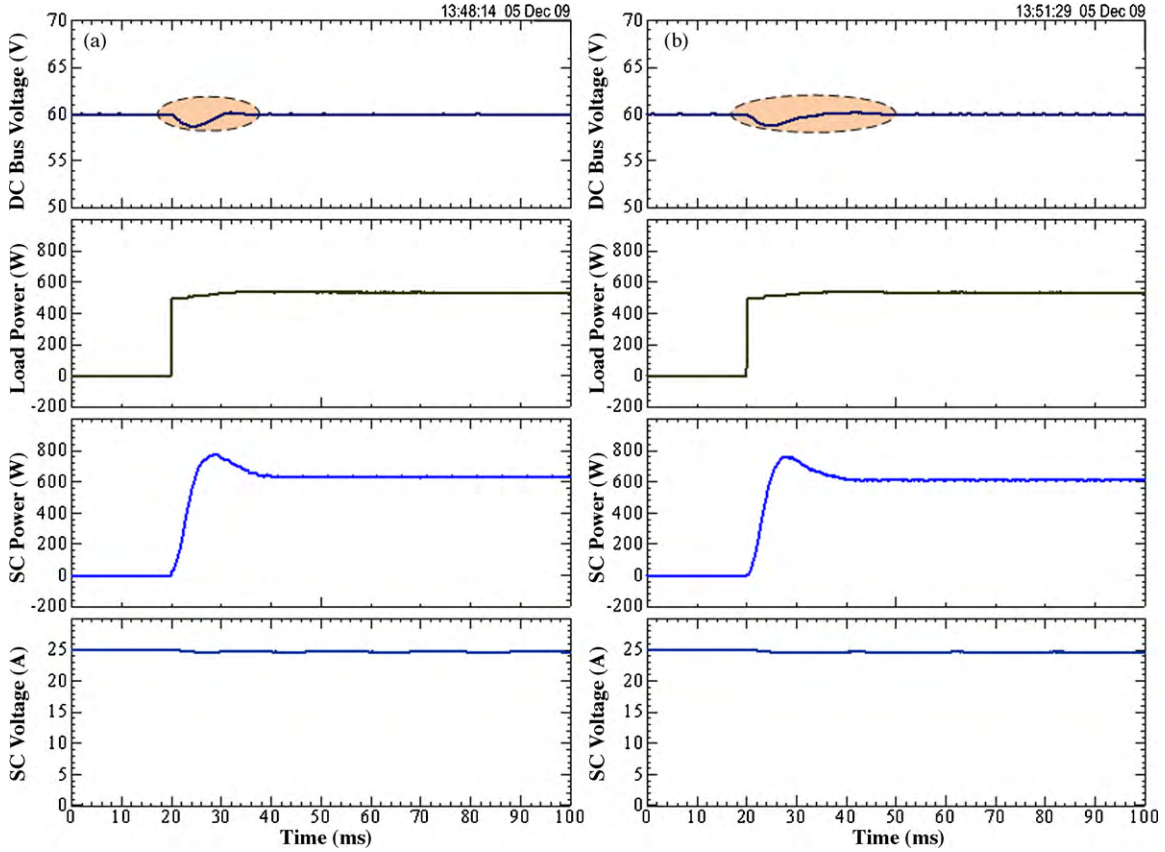

Fig. 9. Comparison of d.c. link stabilization of hybrid energy source during large load step. (a) exact model ($r_{FC} = 0.14\,\Omega$, $r_{Sol} = 0.12\,\Omega$, $r_{SC} = 0.10\,\Omega$) and (b) error model (robustness) ($r_{FC} = 0\,\Omega$, $r_{Sol} = 0\,\Omega$, $r_{SC} = 0\,\Omega$).

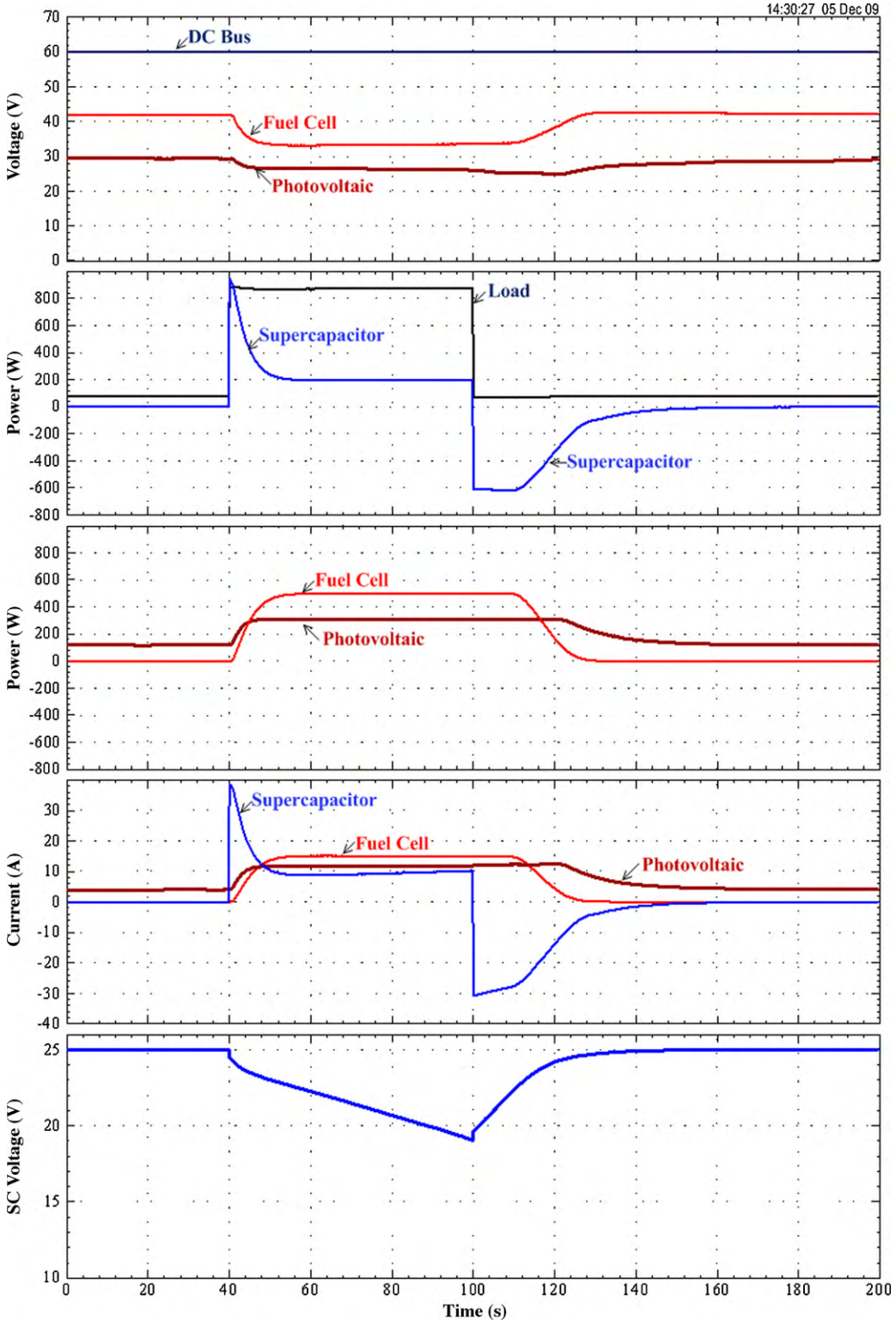

Fig. 10. Hybrid source response during load cycle.

similar to the test bench results in Fig. 10. During the experiment, the FC maximum power was set to 500 W, and the PV maximum power (depending on solar radiation, weather conditions and temperature) was limited by the MPPT. For example, at 15:01:40, the PV maximum power was approximately equal to 180 W; at 15:02:30, the PV maximum power was about 180 W; at 15:03:20, the PV maximum power was around 180 W; and from 15:05:50 to 15:08:20, the PV maximum power was reduced to 0 W, because of the cloudy conditions. In particular, it was found that the power plant was always energy balanced $p_{\mathrm{Load}}(t) \approx p_{\mathrm{FC}}(t) + p_{\mathrm{Sol}}(t) + p_{\mathrm{SC}}(t)$ by the proposed original control algorithm.

The important variable necessary to balance the energy in this complex system is the d.c.-bus energy or voltage. From the experimental validation, the d.c.-bus voltage is automatically controlled at the constant set-point, i.e., $v_{\mathrm{Bus}} = 60$ V. This experiment confirms that the energy in the system is well managed. The fuel cell and

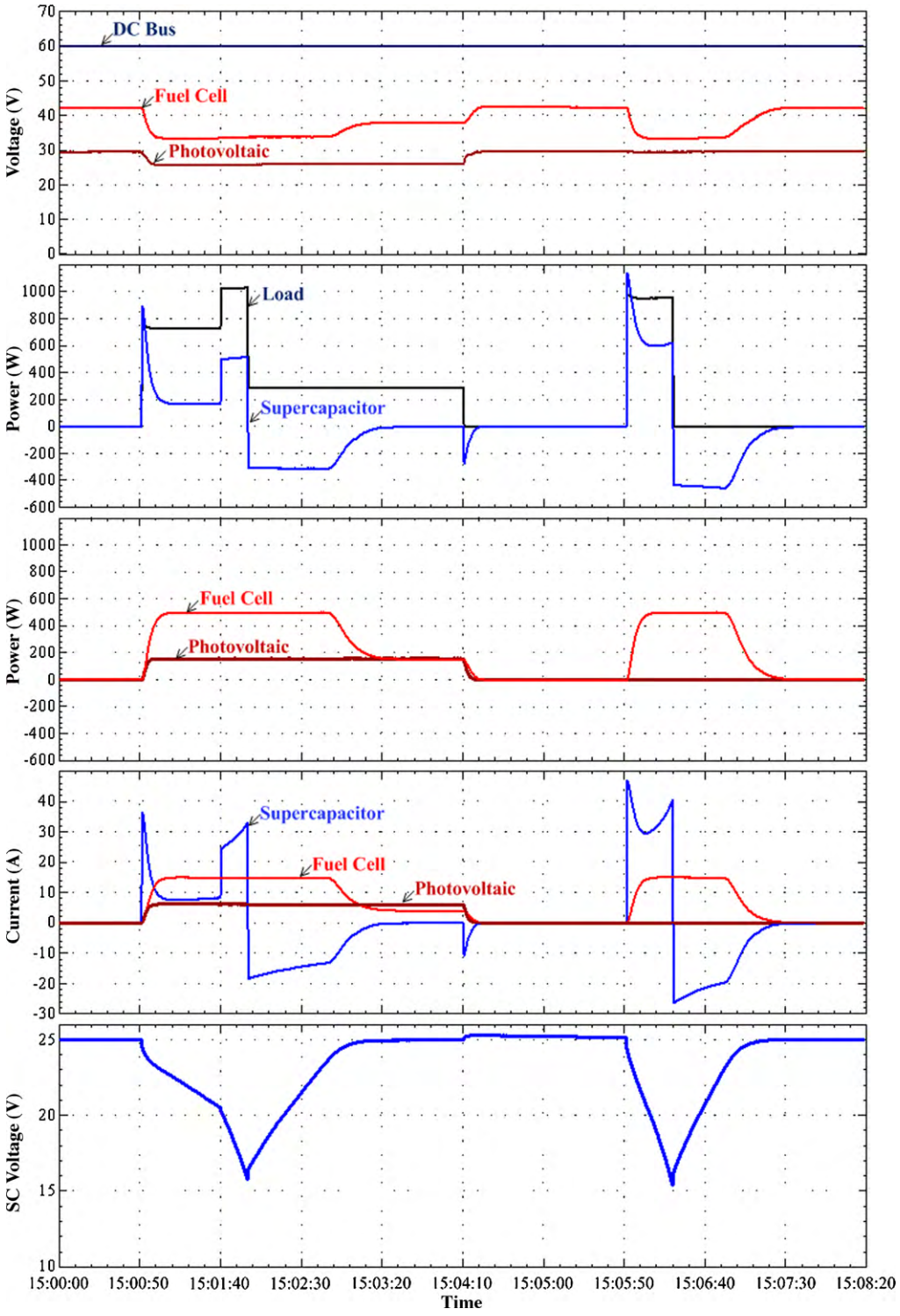

Fig. 11. Hybrid source response during long load cycles.

solar cell powers are limited at their maximum powers, and the fuel cell power dynamics are controlled; as a result, there is no fuel starvation problem and the fuel cell stack lifetime is increased [46–48].

4. Conclusions

Energy management of multi-power sources has been proposed as a solution for a hybrid energy system that uses renewable energy from solar cells, fuel cells and a supercapacitor as an energy storage device. A supercapacitor can advance the load, following the characteristics of the main sources by providing a stronger power response to changes in the system load. During essential steps in the load, the supercapacitor provides the energy balance needed during load transition periods. Adding energy storage to the distributed power systems improves power quality and efficiency.

Experimental verification with a small-scale hybrid test bench (Nexa Ballard fuel cell power generator: 1.2 kW, 46 A; Ekarat Solar Cell power module: 800 W, 31 A; Maxwell supercapacitor storage device: 100 F, 32 V) has demonstrated the excellent performance of

the whole system, and has validated the proposed energy management principle.

Acknowledgments

The authors gratefully acknowledge the French National Center for Scientific Research (CNRS), the Groupe de Recherche en Electrotechnique et Electronique de Nancy (GREEN: UMR 7037), the Thailand Research Fund (TRF Grant number: MRG5180348), and the Thai-French Innovation Institute (TFII) for supporting this project. The research work was undertaken in the "Franco-Thai Cooperation Program in Higher Education and Research Year: 2009–2011".

References

[1] R. Toonssen, N. Woudstra, A.H.M. Verkooijen, J. Power Sources 194 (October (1)) (2009) 456–466.
[2] K. Rajashekara, J. Grieve, D. Daggett, IEEE Ind. Appl. Mag. 14 (July–August (4)) (2008) 54–60.
[3] N.W. Miller, D. Guru, K. Clark, IEEE Ind. Appl. Mag. 14 (March–April (4)) (2009) 54–61.
[4] A. Bergen, L. Pitt, A. Rowe, P. Wild, N. Djilali, J. Power Sources 186 (2009) 158–166.
[5] G.S. Aglietti, S. Redi, A.R. Tatnall, T. Markvart, IEEE Trans. Energy Convers. 24 (June (2)) (2009) 442–451.
[6] H. Patel, V. Agarwal, IEEE Trans. Energy Convers. 24 (March (1)) (2009) 256–263.
[7] J.R. Salgado, M.A.D. Aguilar, J. Power Sources 186 (2009) 455–463.
[8] J.P. Mock, S.A. Schmid, J. Power Sources 190 (2009) 133–140.
[9] P. Thounthong, B. Davat, S. Raël, P. Sethakul, IEEE Ind. Appl. Mag. 15 (July–August (4)) (2009) 52–59.
[10] P. Corbo, F. Migliardini, O. Veneri, J. Power Sources 181 (July) (2008) 363–370.
[11] M. Kolhe, IEEE Trans. Energy Convers. 24 (June (2)) (2009) 511–519.
[12] T. Senjyu, M. Datta, A. Yona, C.H. Kim, IEEE Trans. Energy Convers. 24 (June (2)) (2009) 520–528.
[13] A.J. del Real, A. Arce, C. Bordons, J. Power Sources 193 (2009) 315–321.
[14] P. Thounthong, S. Raël, B. Davat, IEEE Trans. Energy Convers. 23 (January (1)) (2008) 148–155.
[15] N. Kakimoto, H. Satoh, S. Takayama, K. Nakamura, IEEE Trans. Energy Convers. 24 (June (2)) (2009) 465–473.
[16] A. Cooper, J. Furakawa, L. Lam, M. Kellaway, J. Power Sources 188 (2009) 642–649.
[17] P. Thounthong, V. Chunkag, P. Sethakul, B. Davat, M. Hinaje, IEEE Trans. Veh. Technol. 58 (8) (Oct. 2009) 3892–3904.
[18] E. Schaltz, A. Khaligh, P.O. Rasmussen, IEEE Trans. Veh. Technol. 58 (8) (Oct. 2009) 3882–3891.
[19] J. Bernard, S. Delprat, F.N. Büchi, T.M. Guerra, IEEE Trans. Veh. Technol. 58 (September (7)) (2009) 3168–3176.
[20] J. Bauman, M. Kazerani, IEEE Trans. Veh. Technol. 58 (September (7)) (2009) 3186–3197.
[21] P. Thounthong, S. Raël, B. Davat, IEEE Trans. Ind. Electron. 54 (December (6)) (2007) 3225–3233.
[22] S.J. Chiang, H.J. Shieh, M.C. Chen, IEEE Trans. Ind. Electron. 56 (November (11)) (2009) 4344–4353.
[23] A.F. Segura, E. Durán, J.M. Andújar, J. Power Sources 193 (2009) 276–284.
[24] M. Ferraro, F. Sergi, G. Brunaccini, G. Dispenza, L. Andaloro, V. Antonucci, J. Power Sources 193 (2009) 342–348.
[25] A.E. Auld, J. Brouwer, K.M. Smedley, S. Samuelsen, IEEE Trans. Energy Convers. 24 (September (3)) (2009) 617–625.
[26] P. Thounthong, S. Raël, IEEE Ind. Electron. Mag. 3 (September (3)) (2009) 25–37.
[27] Y. Lembeye, V.D. Bang, G. Lefèvre, J.P. Ferrieux, IEEE Trans. Energy Convers. 24 (March (1)) (2009) 203–210.
[28] S.Y. Choe, J.W. Ahn, J.G. Lee, S.H. Baek, IEEE Trans. Energy Convers. 23 (June (2)) (2008) 669–680.
[29] P. Thounthong, B. Davat, S. Raël, P. Sethakul, IEEE Ind. Electron. Mag. 3 (March (1)) (2009) 32–46.
[30] S.M. Muyeen, R. Takahashi, T. Murata, J. Tamura, IEEE Trans. Energy Convers. 24 (September (3)) (2009) 740–749.
[31] D. Feroldi, M. Serra, J. Riera, J. Power Sources 190 (2009) 387–401.
[32] A. Payman, S. Pierfederici, F. Meibody-Tabar, Energy Convers. Manage. 49 (June (6)) (2008) 1637–1644.
[33] P. Thounthong, S. Raël, B. Davat, IEEE Trans. Energy Convers. 24 (March (1)) (2009) 247–255.
[34] P. Thounthong, S. Raël, B. Davat, J. Power Sources 193 (August (1)) (2009) 376–385.
[35] R. Nozu, M. Iizuka, M. Nakanishi, M. Kotani, J. Power Sources 186 (2009) 570–579.
[36] M.A. Danzer, J. Wilhelm, H. Aschemann, E.P. Hofer, J. Power Sources 176 (2008) 515–522.
[37] H. Aschemann, D. Schindele, IEEE Trans. Ind. Electron. 55 (November (11)) (2008) 3855–3864.
[38] A. Gensior, H. Sira-Ramírez, J. Rudolph, H. Güldner, IEEE Trans. Ind. Electron. 56 (February (2)) (2009) 360–370.
[39] M. Fliess, J. Lévine, Ph. Martin, P. Rouchon, Int. J. Control. 61 (6) (1995) 1327–1361.
[40] M. Fliess, J. Lévine, Ph. Martin, P. Rouchon, IEEE Trans. Automat. Control. 44 (May (5)) (1999) 922–937.
[41] C.P. Mudannayake, M.F. Rahman, IEEE Ind. Appl. Mag. 15 (July–August (4)) (2009) 14–25.
[42] S. Lalouni, D. Rekioua, T. Rekioua, E. Matagne, J. Power Sources 193 (2009) 899–907.
[43] G. Carannante, C. Fraddanno, M. Pagano, L. Piegari, IEEE Trans. Ind. Electron. 56 (November (11)) (2009) 4374–4380.
[44] N. Femia, G. Petrone, G. Spagnuolo, M. Vitelli, IEEE Trans. Ind. Electron. 56 (November (11)) (2009) 4473–4482.
[45] D.J. Perreault, J.G. Kassakian, IEEE Trans. Circuits Syst. I, Fundam. Theory Appl. 44 (August (8)) (1997) 728–734.
[46] N. Yousfi-Steiner, Ph. Moçotéguy, D. Candusso, D. Hissel, J. Power Sources 194 (October (1)) (2009) 130–145.
[47] J. Hasikos, H. Sarimveis, P.L. Zervas, N.C. Markatos, J. Power Sources 193 (August (1)) (2009) 258–268.
[48] F. Ettingshausen, J. Kleemann, M. Michel, M. Quintus, H. Fuess, C. Roth, J. Power Sources 194 (December (2)) (2009) 899–907.